

## 6 DEVELOPMENT OF AN IR SIGNATURE MODEL

### 6.1 Introduction

Signature prediction is an important part of infrared system analysis. IR signature simulation provides a very cost effective means to examine a wide range of scenarios. The complexities of IR computation are such that many large computer models have been constructed for this purpose, and ultimately for careful analysis, there are no substitutes for complex numerical techniques. However, simple analytical techniques derived from first principles can be applied that may provide a lower level of fidelity and accuracy, but may be adequate for a specific purpose [DUD93].

The objective of this chapter is to provide a description of the factors affecting the IR signature of a scene. To discuss the steps involved in the development of IR signature models of the targets, the background and flares. Also, the effects of the atmosphere on the IR radiations are modelled using LOWTRAN atmospheric transmission code. The missile seeker/detector and optics modelling is discussed. The power received at the detector is modelled to estimate the lock-on range of a heat seeking missile. At the end of this chapter, the ways to increase the fidelity of the model are discussed.

### 6.2 IR Signature Modelling of the Background

In an IR scene the background may consist of one uniform background such as clear sky or a combination of different sub-backgrounds. The backgrounds can be sky, ground, desert, concrete, woodland etc. The background is modelled as a graybody. The radiance of the background is calculated from the temperature and the emissivity. The total radiance received at the detector is calculated after considering the atmospheric transmission ( $\tau_a$ ). The total spectral radiance is calculated by summing the values over the detector waveband. In the case of a missile/target engagement simulation, the total background radiance is calculated at every frame or after a time interval ( $\Delta t$ ).

#### 6.2.1 Background Input Parameters

The input data for calculating the background radiance can be selected from lookup tables stored in Microsoft Excel spreadsheets or entered manually in the main

programme. Table 6-1 shows the typical values of the emissivity (total normal) and temperature of various background materials presently fed in lookup tables. However, data for several other background materials can be stored in the same spreadsheet. The following input parameters are required for modelling the background.

- (a) Emissivity of the background material,
- (b) Temperature of the background in Kelvin,
- (c) Area of the background in square-meters, and
- (d) Range of the background from the detector in kilometres

**Table 6-1 : Background input parameters (Source [HUD69])**

| Material          | Emissivity | Temperature (K) |
|-------------------|------------|-----------------|
| RED BRICK         | 0.93       | 293.15          |
| CONCRETE          | 0.92       | 293.15          |
| SAND              | 0.90       | 293.15          |
| WOOD (PLANED OAK) | 0.90       | 293.15          |
| WATER (DISTILLED) | 0.96       | 293.15          |
| OIL PAINT         | 0.94       | 373.15          |
| SNOW              | 0.85       | 263.15          |

### 6.2.2 Sky-radiance Data Sets

In the case of air-to-air or surface-to-air missiles, the background may be sky only. The sky-radiance data for a number of weather conditions and altitudes is generated by running the LOWTRAN atmospheric transmission code. Table 6-2 shows various inputs to be fed in to LOWTRAN for calculating the sky-radiance [LOW89]. This table shows the three sets of inputs which may represent “good”, “typical” and “bad” weather conditions. The spectral band is kept from 1 to 15 microns which covers most IR heat seeking missiles [JOS93]. To calculate the sky-radiance as a background, the path-length may be kept as a big number (such as 200 km) to get sufficient range of the sky behind the aerial target. The path-type is kept as horizontal for the air-to-air mode and for surface-to-air mode it could be selected as slant-path. The sky-radiance is calculated for different altitudes and weather conditions and stored in an Excel spreadsheet as lookup tables. For the selected weather condition, waveband and altitude, the desired sky-radiance data is called into the main programme. Figure 6-1 shows sky-radiance data at various altitudes for a “good” atmosphere calculated by running LOWTRAN. The sky-radiance data for several more weather conditions and

altitudes may be calculated in similar way using LOWTRAN code and stored in the same Excel spreadsheet. These look-up tables are stored outside the main programme and only the corresponding data column relating to the desired weather conditions, altitude and waveband is extracted. This makes the main programme more efficient and less bulky.

**Table 6-2 : Typical LOWTRAN input parameters for calculating sky-radiance**

| PARAMETER/ATMOSPHERE TYPE            | GOOD                              | TYPICAL                  | BAD                     |
|--------------------------------------|-----------------------------------|--------------------------|-------------------------|
| MODEL ATMOSPHERE                     | 1976 US Standard                  |                          |                         |
| TYPE OF ATMOSPHERIC PATH             | Horizontal Path                   |                          |                         |
| MODE OF EXECUTION                    | Radiance                          |                          |                         |
| EXECUTED WITH MULTIPLE SCATTERING    | No                                |                          |                         |
| AEROSOL MODEL USED                   | No aerosol attenuation            | Rural-Visibility = 23 km | Rural-Visibility = 5 km |
| UPPER ATMOSPHERE AEROSOLS            | Background Stratospheric          |                          |                         |
| CLOUD/RAIN AEROSOL EXTENSIONS        | No Cloud or Rain                  | No Cloud or Rain         | Cumulus Clouds          |
| RAIN RATE (mm/hour)                  | 0                                 | 0                        | 2 mm/hour               |
| GROUND ALT ABOVE SEA LEVEL (km)      | 0                                 |                          |                         |
| INITIAL ALTITUDE (km)                | 0                                 |                          |                         |
| FINAL ALTITUDE (km)                  | 0                                 |                          |                         |
| INITIAL ZENITH ANGLE (degrees)       | 0                                 |                          |                         |
| PATH LENGTH (km)                     | 200                               |                          |                         |
| SHORT PATH-0/ LONG PATH-1            | 1                                 |                          |                         |
| INITIAL FREQUENCY (wavenumber)       | 665 (15.038 micron)               |                          |                         |
| FINAL FREQUENCY (wavenumber)         | 10000 (1 micron)                  |                          |                         |
| FREQUENCY INCREMENT (wavenumber)     | 5                                 |                          |                         |
| NUMBER ON PLOTS                      | 1                                 |                          |                         |
| HARD COPY OPTION                     | 1-generate print / printer output |                          |                         |
| INTERACTIVE GRAPHICS MODE            | 6- 640x350 dot Mode               |                          |                         |
| PLOT TYPE                            | 0-Radiance in micron              |                          |                         |
| LENGTH OF X-AXIS (in inches)         | 7 inches                          |                          |                         |
| BEGINNING WAVENUMBER/wavelength (µm) | 665/1.00                          |                          |                         |
| ENDING WAVENUMBER/wavelength (µm)    | 10000/15.00                       |                          |                         |
| LENGTH OF Y-AXIS (in inches)         | 6 inches                          |                          |                         |
| MINIMUM RADIANCE                     | 0                                 |                          |                         |
| MAXIMUM RADIANCE                     | 1                                 |                          |                         |
| Y-Axis Annotation Interval           | 0.1                               |                          |                         |
| LINE TYPE                            | 1 (normal line)                   |                          |                         |

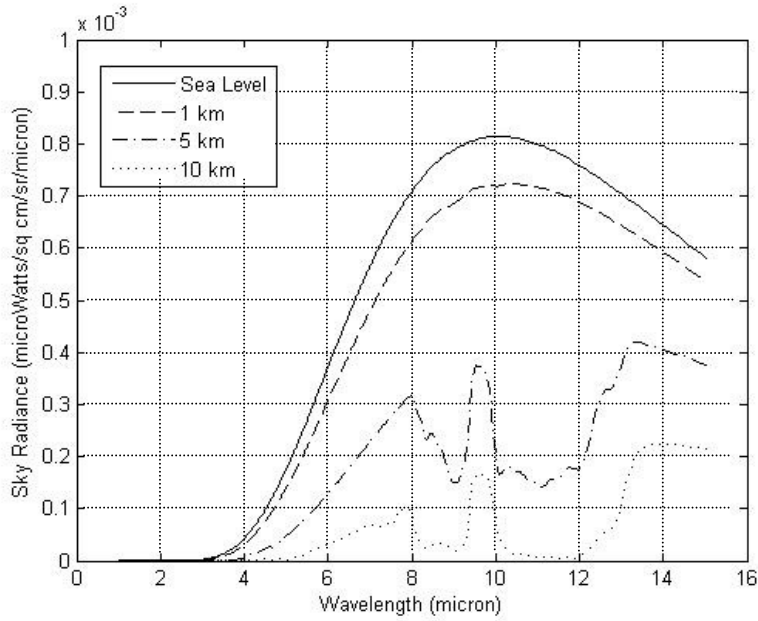


Figure 6-1 : Sky-radiance in good weather for various altitudes

### 6.2.3 Calculating Background Radiance

The spectral distribution and magnitude of an object's IR radiation are primarily a function of the object's temperature and emissivity. For the given emissivity and the temperature, the background radiance can be calculated using the Planck's radiation law equation given in Chapter-2 as Equation 2-7. The same is rewritten as Equation 6-1 for background spectral radiance. The total spectral radiation, over the detector waveband, is found by first calculating the radiance values for every 0.01  $\mu\text{m}$  by using Equation 6-1. The outputs are stored as an array of radiance values at every 0.01  $\mu\text{m}$  interval. For multiple backgrounds, the radiance of each sub-background is to be calculated separately.

$$N_B = \frac{1}{\pi} \int_{\lambda_1}^{\lambda_2} \frac{\epsilon_B \cdot c_1}{\lambda^5 \left( e^{\left[ \frac{c_2}{\lambda \cdot T_B} \right]} - 1 \right)} d\lambda \quad (6-1)$$

Where,

$N_B$  is the radiance of the background,

$T_B$  is the temperature of the background,

$\epsilon_B$  is the total emissivity of the background material,

$\lambda_1$  and  $\lambda_2$  are the detector waveband start and stop wavelengths,

$c_1$  and  $c_2$  are the first and second radiation constants respectively.

#### 6.2.4 Multiple Backgrounds or Sub-backgrounds

The total radiance of the background is mainly due to the earth, sky and cloud thermal emissions and (in the day time) the solar reflections. Estimates of atmospheric emission and scattering are quite challenging. Initially, for first-order modelling, only the emissive properties of the background are considered and also the background is considered as one uniform body of constant temperature. However, for airborne targets, the background may be approximated as several horizontal layers of sky and ground [DUD93]. Therefore, to increase the fidelity, the background is modelled as three layers (or planes) of the sky and one layer of the ground. This is achieved by using the “*background*” node of VRML. The details of the physical modelling of the background as layers of sky and ground are explained in Chapter-7 paragraph 7-6. The appearance (colour) of each layer of the ground in the virtual world corresponds to the total radiance of each layer calculated using Equation 6-1. In the case of the sky, the radiance of each layer is extracted from the look-up tables as mentioned in paragraph 6-2-2 above.

However, for the ground targets or very low flying targets, the second order effects such as spatial variations along the mixed background can be modelled by selecting a full 3D environment with multiple backgrounds. Figure 6-2 shows one such scenario of multiple backgrounds in which solid tarmac, grass, ice and mountains, and sky with scattered clouds are all depicted. For higher order modelling of the background, the following parameters are required.

- (a) Temperature of each sub-background
- (b) Emissivity of each sub-background
- (c) Diffused and specular reflectance of each sub-background
- (d) Solar irradiance
- (e) Atmospheric transmittance
- (f) Sky-radiance

The higher order background modelling may be considered in future work for air-to-surface and ground-to-ground modes.

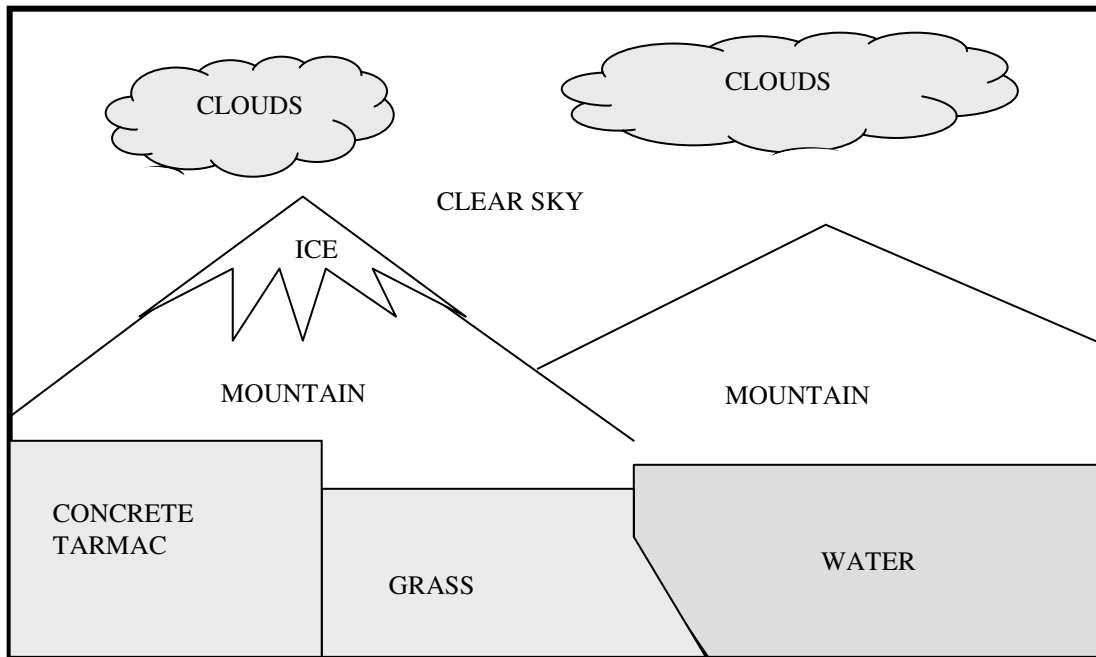


**Figure 6-2 : Sub-backgrounds or multiple-background.**

### **6.3 IR Signature Modelling of the Targets**

Typical military targets are aircraft, tanks, ships or helicopters etc. These are made up of several materials; contain warm surfaces, sources of heat (such as engines) and exhaust gas plume(s). The targets can be modelled as one uniform temperature object or with different temperature zones or sub-targets. Presently, my algorithm can model several different uniform targets or one target with different temperature zones as sub-targets for 2D static analysis of the power received at the detector and lock-on range. For the 3D virtual world, one target with different temperature zones is modelled. The following paragraphs explain the steps involved in the prediction of the IR signature of military targets and the ways to improve the fidelity of the models.

#### **6.3.1 Target Input Parameters**

For IR signature modelling of targets the following parameters of each target or sub-targets are required:

- (a) Emissivity
- (b) Temperature in Kelvin
- (c) Range from the missile in kilometres
- (d) Area in square meters

The input data for several targets is stored in the Microsoft Excel spreadsheet. The data of each required target can be called in or can be fed manually in the main programme. Table 6-3 shows an example of an aircraft data set already stored in the Excel spreadsheet. This data set does not correspond to any specific military aircraft. The data of several targets can be stored in the same spreadsheet.

**Table 6-3 : Target input parameters.**

|              | Area (m <sup>2</sup> ) * | Emissivity | Temperature (K) |
|--------------|--------------------------|------------|-----------------|
| Body         | 30                       | 0.9        | 320             |
| Nose         | 2                        | 0.9        | 350             |
| Leading edge | 1                        | 0.9        | 350             |
| Tail-pipe    | 2                        | 0.9        | 380             |
| Canopy       | 4                        | 0.5        | 250             |
| Plume inner  | 1                        | 0.5        | 1000            |
| Plume outer  | 2                        | 0.5        | 500             |

\* Area is from beam aspect for 2D analysis

### 6.3.2 Calculating Radiance of the Target

The radiance of each target or sub-target is calculated independently. Assuming that the target is a gray-body, radiating uniformly in all directions and knowing the emissivity and the temperature of the object, their radiance is calculated using the Planck's law Equation 2-7. Equation 6-2 shows the integral for calculating the radiance of the target. To solve the integral, the MATLAB function “trapz” is used. This function uses the trapezoidal method of numerical integration [MAT07]. By repeating the integral, the values of radiance at every 0.01 micron step for the entire waveband of the detector are calculated and stored in an array.

$$N_{igt_i} = \frac{1}{\pi} \int_{\lambda_1}^{\lambda_2} \frac{\epsilon_{igt} \cdot c_1}{\lambda^5 \left( e^{\left[ \frac{c_2}{\lambda \cdot T_{igt}} \right]} - 1 \right)} d\lambda \quad (6-2)$$

Where,

$N_{igt_i}$  is the radiance of the target at every 0.01 micron interval

$T_{igt}$  is the temperature of target in Kelvin.

$\epsilon_{igt}$  is the total emissivity of the target.

$\lambda_1$  and  $\lambda_2$  are the start and stop wavelengths for every 0.01 micron step,

$c_1$  and  $c_2$  are the first and second radiation constants respectively.

The target radiance values calculated at every 0.01 micron step are multiplied by the atmospheric transmittance ( $\tau_a$ ) calculated at every 0.01 micron step. The calculation of atmospheric transmittance is discussed in paragraph 6-5. The total radiance over the entire waveband of the detector is calculated by using Equation 6-3.

$$N_{igt} \tau_a = \sum_{i=1}^n (N_{igt_i} \cdot \tau_{a_i}) \quad (6-3)$$

Where,  $N_{igt} \tau_a$  is the total spectral radiance after atmospheric attenuation

$n$  is the number of 0.01 micron intervals in the detector waveband

$N_{igt_i}$  is the target radiance at every 0.01 micron interval

$\tau_{a_i}$  is the atmospheric transmission at every 0.01 micron interval

For the target-missile engagement simulation where the distance between the target and missile is changing constantly, the total spectral radiance ( $N_{igt} \tau_a$ ) calculated in Equation 6-3 is recalculated for every frame.

### 6.3.3 More Realistic Targets with Different Temperature Zones

Initially, for low-fidelity or first-order modelling, the targets were assumed to be a point source with a uniform temperature and emissivity. This may reasonably represent some real targets at longer distances. However, for short ranges and higher-order modelling, the target's thermal profiles should be represented in a more detailed and more realistic manner. For higher-fidelity modelling, the targets are divided into sub-targets based on different temperature zones and radiometric properties. Figure 6-3 shows an example of an aircraft comprising of hot metal parts (engine nozzles), comparatively cold skin, hot exhaust gas plume, leading edges and glass canopy. All these parts have different temperatures and different radiometric properties and may behave differently in the IR band. Similarly, the other military targets, such as a ship, tank and helicopter etc. may also be divided into different sub-targets. The total radiance of each sub-target may be calculated using Equation 6-2 and Equation 6-3.



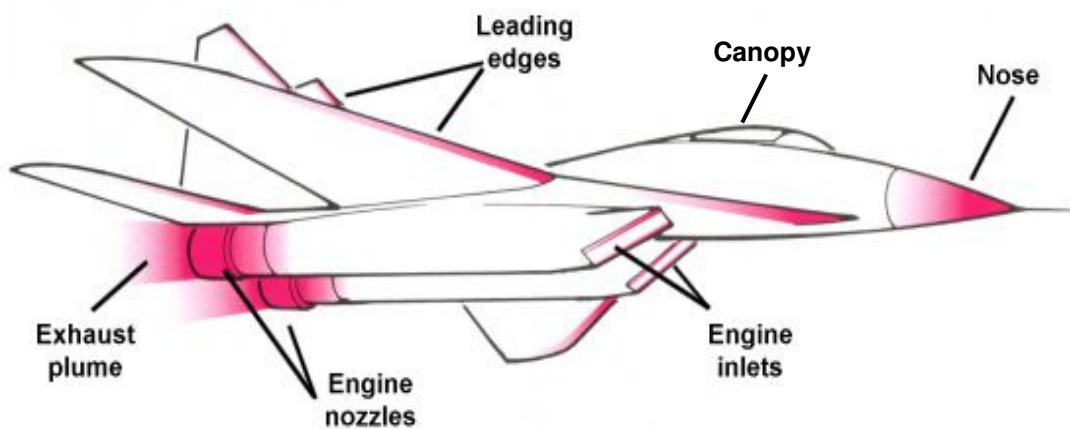


Figure 6-3 : Aircraft thermal radiation sources (source [www.aerospaceweb.org](http://www.aerospaceweb.org))

### 6.3.4 Adding Reflection Effects to the Model

Other than the emissive properties of the targets, their reflective characteristics also contribute to the overall radiance received at the detector. The environmental sources of reflected radiation are the sun, the earth, the sky, atmosphere and clouds. Figure 6-4 shows the typical IR signature elements of an aircraft. Also, in the case of ground or sea targets, the inter-reflections caused by other targets in close vicinity may also contribute towards the overall radiance. However, in the case of airborne targets this may be neglected as aircraft are usually not very close to each other. The total radiance due to the reflections from other sources may be calculated using Equation 6-4 [POL93].

$$N_{reflected} = N_{ss} + N_{es} + N_{sky} + N_{intref} \quad (6-4)$$

Where,  $N_{reflected}$  is the total spectral radiance due to reflection

$N_{ss}$  is the reflected sunshine

$N_{es}$  is either reflected earth shine or cloud shine

$N_{sky}$  is either reflected sky shine or cloud shine

$N_{intref}$  is reflected other targets shine.

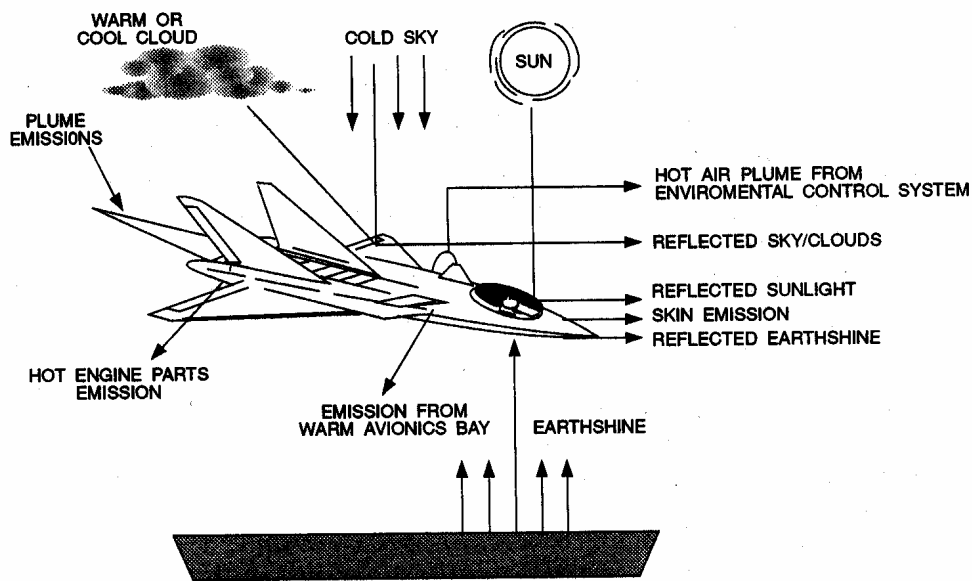


Figure 6-4 : IR signature elements of an aircraft (Source[POL93])

To calculate the total spectral radiance due to reflections, the solar irradiance, earth and sky irradiance are first calculated. The radiance due to reflections depends upon the relative position of the sources, the viewers (seeker) and the angle which they make with the reflecting surface. The reflected radiance has two components, one due to the specular reflectivity and the other due to the diffused reflectivity (due to the scattering) [ZIS93]. Ideally, for true modelling of the physical process, the radiance due to both these components has to be calculated at every point in the scene. However, in the case of dynamic simulations where the position of the target and seeker are changing rapidly, calculating reflected radiance at every point may be computationally expensive. Therefore, to add the effects of reflections on the overall IR signature, I have tried an alternate approach. This may be done by controlling the material properties (appearances) of the objects in virtual world modelling in VRML. The solar, earth, and sky irradiance may be modelled as independent sources and the “*diffusedColor*”, “*ambientIntensity*”, “*ambientColor*” and “*shininess*” used to represent the radiant reflective properties of the material. The details of this approach are explained in Chapter-7 paragraph 7-5-2.

### 6.3.5 Modelling IR Signature of the Exhaust Gas Plume

The exhaust gas plume of an aircraft is usually the dominant source of thermal radiations in the 3 to 5 micron band [DUD93]. The total radiance of an object can have contributions due to emission, transmission and reflection (scattering).

Figure 6-5 shows these three components. The body of a military target is generally solid metal and opaque in nature. We may assume that the “opaque objects” emit thermal radiations and reflect what they receive from the environment. But the transmission part may be neglected [DUD93].

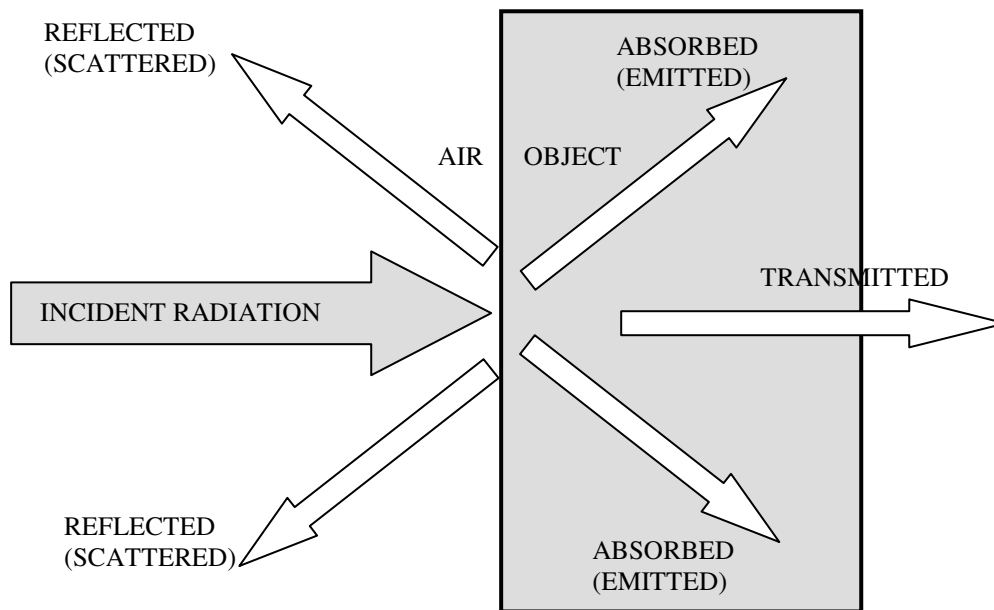


**Figure 6-5 : Transmission, reflection and absorption of thermal radiations.**

On the other hand, the turbine engine exhaust gas plume comprises of the residue leftover from the combustion process and is non-opaque in nature. Thus the exhaust gas plume may be assumed to emit thermal radiations and transmit the energy through a non-opaque volume. But the third element of reflection (or scattering) may be neglected [DUD93]. Therefore, the total radiance of the plume can be represented as given in Equation 6-5.

$$N_{totplume} = N_{plumemis} + \tau_{plume} \cdot N_{behindplume} \quad (6-5)$$

Where,

- $N_{totplume}$  is the total radiance of the plume
- $N_{plumemis}$  is the radiance due to emissive properties of plume
- $N_{behindplume}$  is the radiance of the object behind plume
- $\tau_{plume}$  is the transmittance of the plume

Equation 6-5 has two components, one  $N_{plumemis}$  that is the radiance due to emissive properties of plume. This is similar to the one which is also present in the case of opaque objects. But the other component due to the transmittance is the radiance of objects behind the plume ( $N_{behindplume}$ ) factored with the transmittance of the plume ( $\tau_{plume}$ ). The radiance behind the plume may be that of the target itself, sky or background dependant upon the target aspect or seeker's viewing angle. Calculating the exhaust gas plume radiance is not a simple task. The shape and volume of the plume is not constant. Due to the fast movement of the aircraft and the presence of gases ( $\text{CO}_2$  and  $\text{CO}$ ) in atmosphere, the plume is gradually diluting in the surrounding atmosphere and it is difficult to draw a boundary between the plume and atmosphere. For modelling purpose, the exhaust gas plume may be divided into co-centric cylindrical regions with the same temperature ( $T$ ), pressure ( $P$ ) and molecular density ( $\chi$ ). Although, temperature and other properties are dynamic and vary even within these regions, yet for simplicity they can be considered as constant [DUD93]. Figure 6-6 shows a conceptual model of an exhaust gas plume as co-centric cylindrical regions.

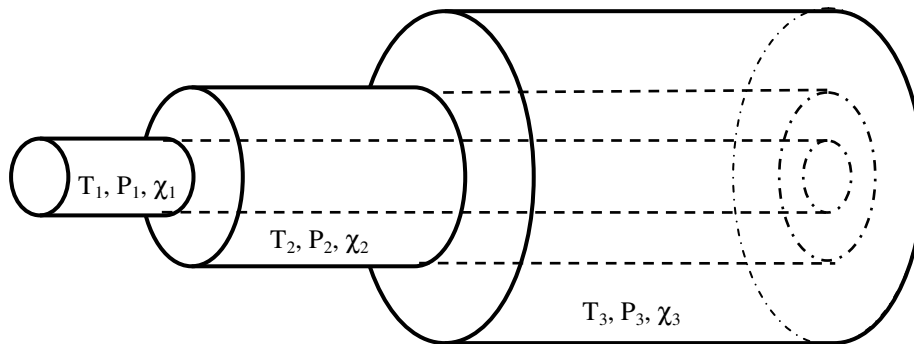


**Figure 6-6 : Exhaust plume modelled as Co-centric cylindrical regions.**

However, for IR signature modelling purpose, the bulk of the radiation of the jet engine exhaust plume comes from the vicinity of the exit plane in a region called the inviscid core. Figure 6-7 shows the inviscid core behind the aircraft engine nozzle. As much as three-quarters of the total plume radiance may be generated within a length of plane shorter than the structural length of the aircraft [DUD93]. The region beyond the inviscid core emits more weakly and is more easily absorbed by the cool atmospheric gases. For IR signature modelling it is important to consider the shape, size and conditions of the hottest exhaust gas region. For a circular nozzle, the

inviscid core may roughly be of cone shape with the base area as that of the nozzle exit area and a length shorter than the aircraft length [DUD93].

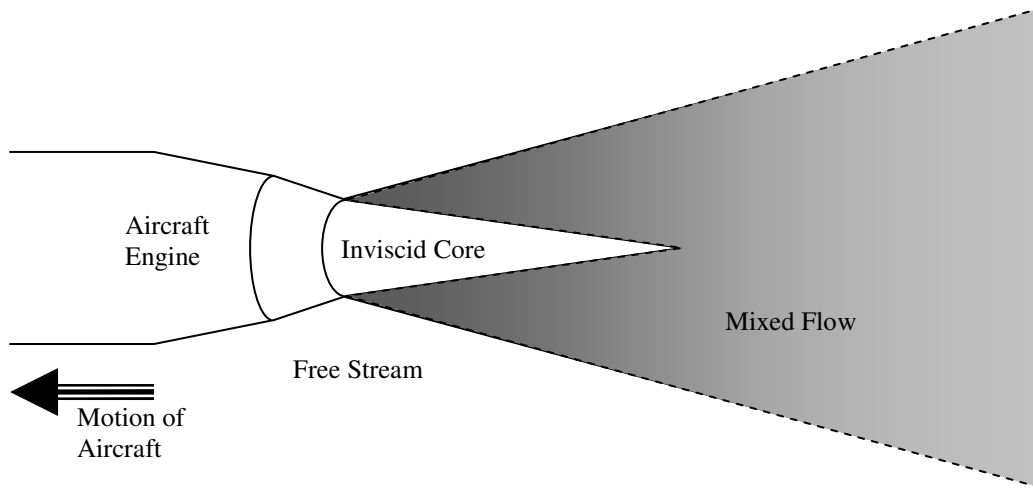


**Figure 6-7 : simplified aircraft jet engine exhaust plume (Source [DUD93])**

In my work, I have modelled the exhaust gas plume inviscide core geometry as two co-centric cones. The inner cone representing a higher temperature as compared to the outer cone. In Equation 6-5, the plume radiance due to the emissive properties ( $N_{plumemis}$ ), may be calculated using the Planck's thermal law Equation 2-7. The radiance of each cone of the plume may be calculated separately using Equation 6-6.

$$N_{plumemis} = \frac{1}{\pi} \int_{\lambda_1}^{\lambda_2} \frac{\epsilon_{\lambda_{plume}} \cdot c_1}{\lambda^5 \left( e^{\left[ \frac{c_2}{\lambda \cdot T_{plume}} \right]} - 1 \right)} d\lambda \quad (6-6)$$

Where,

$T_{plume}$  is the temperature of plume in Kelvin.

$\epsilon_{\lambda_{plume}}$  is the spectral emissivity of the plume.

The spectral emissivity ( $\epsilon_{\lambda_{plume}}$ ) of the plume with spectral resolution of 0.01 micron is stored in a lookup table and can be called in the main programme. Figure 6-8 shows the spectral emissivity of an exhaust gas plume. The  $N_{plumemis}$  for the entire waveband

of the detector is calculated by first calculating the radiance at every 0.01 micron interval using Equation 6-6 and then multiplying it with the atmospheric transmittance ( $\tau_a$ ) calculated at every 0.01 micron. The  $N_{plumemis}\tau_a$  at every 0.01 micron is then summed to calculate to total spectral radiance of the plume due to emissivity.

$$N_{plumemis}\tau_a = \sum_{i=1}^n (N_{plumemis_i} \cdot \tau_{a_i}) \quad (6-7)$$

Where,  $N_{plumemis}\tau_a$  is the plume emissive radiance after atmospheric attenuation,  
 $n$  is the number of 0.01 micron intervals in the detector waveband  
 $N_{plumemis_i}$  is the plume radiance due to emissivity at every 0.01 micron interval  
 $\tau_{a_i}$  is the atmospheric transmittance at every 0.01 micron step

For the dynamic target-missile engagement simulation, where the distance between the target and missile is changing, the product ( $N_{plumemis}\tau_a$ ) is to be calculated at each time interval or frame. The other component of plume radiance due to the transmittance as shown in Equation 6-5, may be calculated by multiplying the plume transmittance ( $\tau_{plume}$ ) with the radiance of the object behind the plume ( $N_{behindplume}$ ). For one static scene, this may be simple, however, for the target missile engagement simulation, where the aspect angle is changing in every frame; the  $N_{behindplume}$  will keep on changing and may be difficult to calculate for every frame. However, as an alternate approach, the plume radiance due to the transmission may be modelled by using the “*transparency*” feature of the VRML material field. This is achieved by making the two cones of the plume semi-transparent. The value of the “*transparency*” may be calculated from Equation 6-8 assuming that the radiance due to reflection is negligible. The details of geometrical modelling of the exhaust gas plume as a semi-transparent object are discussed in Chapter-7 paragraph 7-5-5.

$$\tau_{plume} = 1 - \epsilon_{plume} \quad (6-8)$$

Where,  $\tau_{plume}$  is the transmittance of the plume, and  
 $\epsilon_{plume}$  is the total emissivity of the plume.

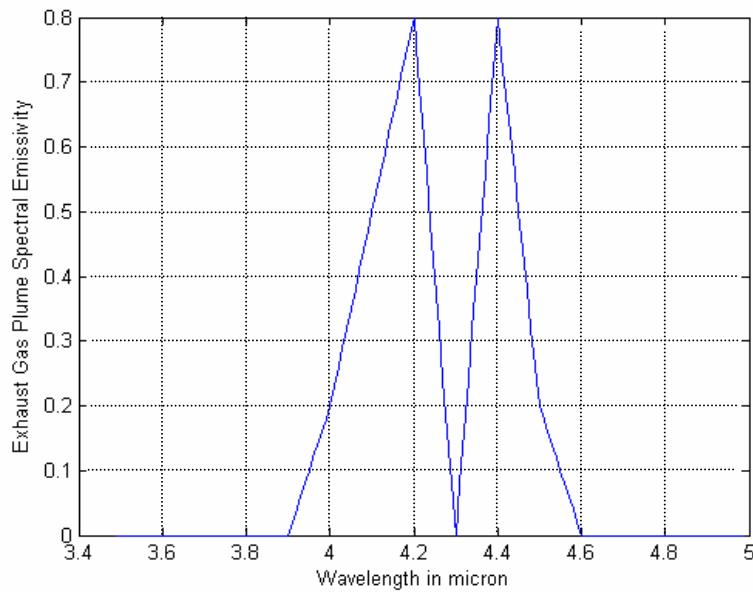


**Figure 6-8 : Spectral emissivity of the exhaust gas plume**

#### **6.4 IR Signature Modelling of IRCM (Flares)**

The IR flares dispensed by military targets, are another source of IR radiation. The IR energy radiating from the flare is also part of the overall IR signature of the scene. The IR signature of a flare in the scene depends upon the physical shape of the flare, the dispensation sequence, ballistic trajectory and the irradiance properties of the flare material. In this chapter, only the spectral radiance and temporal response is modelled. The physical aspect of flare modelling is covered in detail in Chapter-7 paragraph 7-10.

Ideally, the IR signature of a flare should be spectrally and spatially matched that of the platform to be protected but with a higher radiant intensity, however, conventional flares act like a hot point source. Therefore, conventional flares may be modelled as a point source with a higher temperature (typically above 2000 K) [POL93]. In this work the spectral and temporal characteristics of the flare are modelled.

##### **6.4.1 Input Data Required for Flare IR Signature Modelling**

For the flare IR signature modelling the following parameters are required as inputs:

- (a) Flare rise time ( $t_{rise}$ ),

- (b) Flare burn time ( $t_{burn}$ ),
- (c) Burn time constant ( $\tau_{burn}$ ),
- (d) Rise time constant ( $\tau_{rise}$ ),
- (e) Temperature of the flare ( $T_{flare}$ ),
- (f) Emissivity of the flare ( $\epsilon_{flare}$ ).

#### 6.4.2 Assumptions for Modelling Flare IR Signature

The effects of altitude and the wind stream on the flare intensity are important and degrade the overall radiant intensity of the flare. However, at this stage, to keep the model simple, the effect of altitude and the wind stream on the IR signature are not considered. Also, the spectral summing is performed after the detector and optics; this implies that the spectral response of the detector and optics is not modelled. However, these may be considered in future work.

#### 6.4.3 Modelling IR Spectral Response of Flare

For IR signature modelling purposes a full flare plume could be modelled as several cones of different temperature zones or several disc of different temperature. The details of 3D shape modelling of the flare plume are given in Chapter-7. Presently, the flare plume geometry is modelled as two co-centric cones with different temperatures. Figure 6-9 shows the geometry of the flare plume. The inner zone has a higher temperature than the outer zone. The spectral radiance of each zone of the flare plume is calculated by using the Planck's radiation law Equation 2-7. Equation 6-9 shows the integral for calculating the spectral radiance of the flare.

$$N_{flare} = \frac{1}{\pi} \int_{\lambda_1}^{\lambda_2} \frac{\epsilon_{flare} \cdot c_1}{\lambda^5 \left( e^{\left[ \frac{c_2}{\lambda \cdot T_{flare}} \right]} - 1 \right)} d\lambda \quad (6-9)$$

Where,

$T_{flare}$  is the temperature of flare in Kelvin.

$\epsilon_{flare}$  is the emissivity of the flare.

The total radiance of the flare after atmospheric attenuation is calculated by multiplying the flare radiance ( $N_{flare}$ ) calculated at every 0.01 micron step in Equation 6-9 with the atmospheric transmittance ( $\tau_a$ ) measured at every 0.01 micron step. To



calculate the total spectral radiance, the product ( $N_{flare} \times \tau_a$ ) is summed over entire waveband of the detector as given in Equation 6-10.

$$N_{flare} \tau_a = \sum_{i=1}^n (N_{flare_i} \cdot \tau_{a_i}) \quad (6-10)$$

Where, “ $n$ ” is the number of 0.01 micron intervals in waveband,

$N_{flare_i}$  is the flare radiance at every 0.01 micron interval,

$\tau_{a_i}$  is the atmospheric transmission at every 0.01 micron interval.

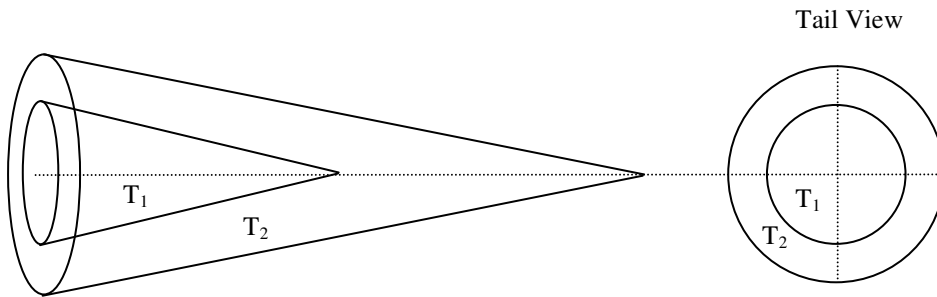


**Figure 6-9 : IR flare plume modelled as co-centric cones**

To observe the effects of the inner cone signature, the outer layers are modelled as the semi-transparent so the inner cone signature can propagate out through the outer cone.

#### 6.4.4 Modelling Temporal Response of IR Flare

Unlike targets and background, the flare’s source of radiation is not permanent (in reference to the missile/target engagement time). Therefore, the flare’s radiant intensity will vary with respect to time. The temporal response of the flare may be modelled as an exponential rise and decay over the time [VAI96]. The total flare radiance calculated after atmospheric effects in Equation 6-10 is multiplied with an exponential function  $f(t)$ . The temporal response of the flare radiance  $N_{flare}(t)$  is modelled as in Equation 6-11.

$$N_{flare}(t) = N_{flare} \tau_a \cdot f(t) \quad (6-11)$$

$$f(t) = 1 - e^{-t/\tau_r}, \quad 0 \leq t \leq t_r$$

$$f(t) = e^{-(t-t_r)/\tau_b}, \quad t_r \leq t \leq t_b$$

Where,

$N_{flare}\tau_a$  is the total radiance of the flare after atmospheric attenuation,

$t_r$  is rise time in seconds,

$t_b$  is the burn time in seconds,

$\tau_r$  is the rise time constant,

$\tau_b$  is the burn time constant.

The function  $f(t) = 1 - e^{-t/\tau_r}$  given in Equation 6-11 represents the rise curve and the function  $f(t) = e^{-t/\tau_b}$  represent the decay. Figure 6-10 shows an example of the temporal response of the flare plotted for one set of input values. The shape of the rise and decay curves may be controlled by varying the respective time constants. The function  $f(t)$  in Equation 6-11 starts at zero time (i.e. assuming that the flare is ejected at  $t = 0$ ). The time ( $t$ ) represent the time of simulation running with  $t = 0$  as the start of the simulation. Therefore, to consider flare ejection at any time during the simulation, or in the case of multiple flare ejections, the flare eject time ( $t_{eject}$ ) is added in the  $f(t)$  in Equation 6-11 and rewritten as Equation 6-12.

$$N_{flare}(t) = N_{flare}\tau_a \cdot f(t) \quad (6-12)$$

$$f(t) = 1 - e^{-t/(\tau_r + t_{eject})}, \quad t_{eject} \leq t \leq (t_r + t_{eject})$$

$$f(t) = e^{-\frac{-(t - (t_r + t_{eject}))}{\tau_b + t_{eject}}}, \quad (t_r + t_{eject}) \leq t \leq (t_b + t_{eject})$$

Where,  $t_{eject}$  is the time at which flare ejects after the start of the simulation.

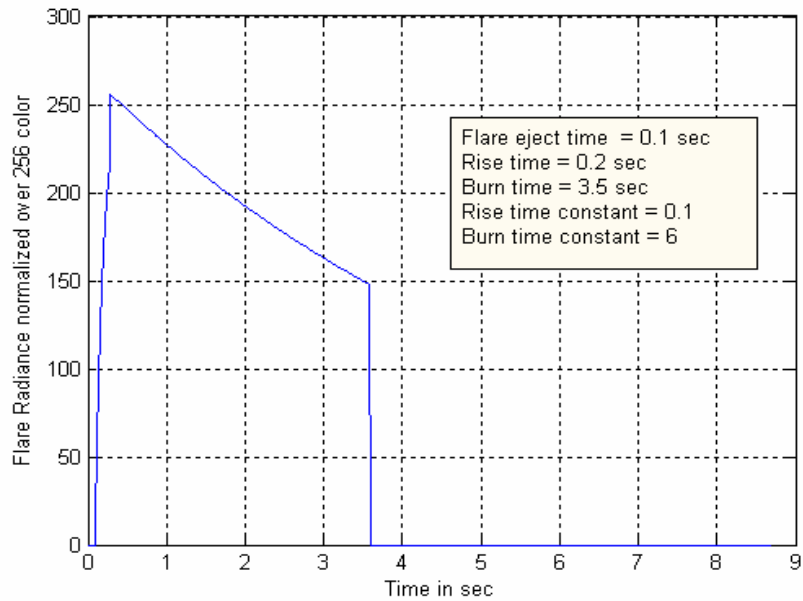


**Figure 6-10 : Temporal response of flare**

### 6.5 Modelling Atmospheric Effects on IR Signature

All IR systems are susceptible to the atmospheric conditions. The different weather conditions could be: clear sky, haze, fog, rain or snow etc. For higher-order IR signature modelling, the attenuation caused by the propagation of the IR energy through the atmosphere is to be considered. In this work, the LOWTRAN atmospheric propagation code is used for modelling the atmospheric transmittance and the path radiance. LOWTRAN is a DOS based code which requires many inputs to be fed in to calculate transmittance values for the desired spectral band. Also for missile/target engagement simulations the transmittance values at different ranges and altitudes are required. Thus by running LOWTRAN several times the transmittance data for different weather conditions and altitudes are calculated and stored as look-up tables as a function of wavelength. The data is stored in Microsoft Excel spreadsheets. Each column represents transmittance values for one set of weather conditions or altitude. Table 6-4 shows three sets of weather conditions for which the transmittance data is calculated using LOWTRAN. However, the transmittance data for any number of weather conditions and altitude can be calculated and stored in the same Excel spreadsheet. The look-up tables are stored outside the main programme and only the data column related to the desired weather condition, altitude and waveband of the seeker is called in the main programme.

**Table 6-4 : LOWTRAN inputs for three weather conditions**

| PARAMETER          | GOOD                   | TYPICAL               | BAD                  |
|--------------------|------------------------|-----------------------|----------------------|
| Aerosol model used | No aerosol attenuation | Rural visibility 23km | Rural visibility 5km |
| Clouds / Rain      | No clouds or rain      | No cloud or rain      | Cumulus clouds       |
| Rain rate          | 0                      | 0                     | 2 mm/hour            |

### 6.5.1 Inputs Required to Generate Atmospheric Transmission Data

Table 6-5 lists the typical LOWTRAN input parameters required to calculate the atmospheric transmission data [LOW89]. By selecting different altitudes, path types, weather conditions and model atmosphere values, several sets of transmission data can be generated. Figure 6-11 shows the atmospheric transmission of 1 km horizontal path-length, at an altitude of 1 km calculated by LOWTRAN for “good”, “typical” and “bad” weather conditions.

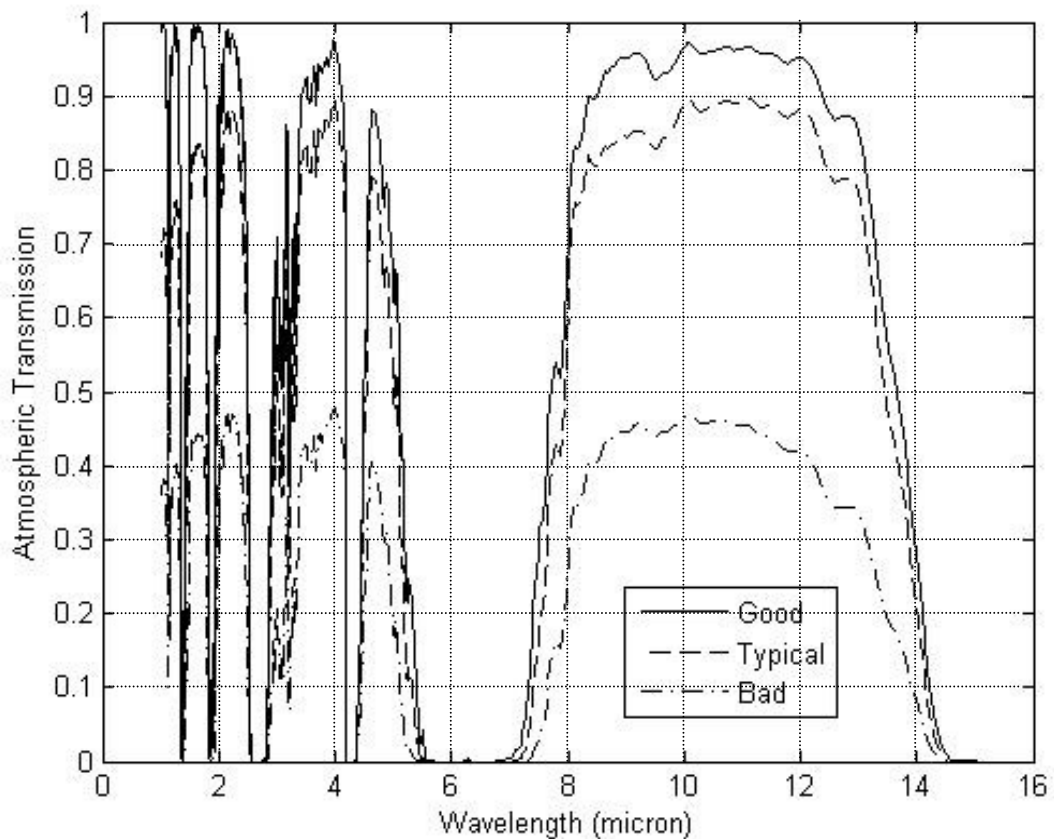


**Figure 6-11 : Atmospheric transmission of 1 km path length**

**Table 6-5 : LOWTRAN inputs to calculate atmospheric transmittance**

| PARAMETER  | GOOD  | TYPICAL          | BAD            |
|--|---|------------------|----------------|
| MODEL ATMOSPHERE                                 | 1976 US Standard                                  |                  |                |
| TYPE OF ATMOSPHERIC PATH                         | Horizontal Path                                   |                  |                |
| MODE OF EXECUTION                                | Transmittance                                     |                  |                |
| EXECUTED WITH MULTIPLE SCATTERING                | No  |                  |                |
| AEROSOL MODEL USED                               | NO Aerosol Atten                                  | Rural-VIS=23km   | Rural-VIS=5km  |
| UPPER ATMOSPHERE AEROSOLS                        | Background Stratospheric                          |                  |                |
| CLOUD/RAIN AEROSOL EXTENSIONS                    | No Cloud or Rain                                  | No Cloud or Rain | Cumulus Clouds |
| RAIN RATE (mm/hour)                              | 0   | 0                | 2mm            |
| GROUND ALT ABOVE SEA LEVEL (km)                  | 0   |                  |                |
| INITIAL ALTITUDE (km)                            | 1 km  |                  |                |
| FINAL ALTITUDE (km)                              | 1 km  |                  |                |
| INITIAL ZENITH ANGLE (degrees)                   | 0   |                  |                |
| PATH LENGTH (km)                                 | 1 km  |                  |                |
| SHORT PATH-0/ LONG PATH-1                        | 0   |                  |                |
| INITIAL FREQUENCY (wavenumber)                   | 665 (=15 MICRONS)                                 |                  |                |
| FINAL FREQUENCY (wavenumber)                     | 10000 (=1 MICRON)                                 |                  |                |
| FREQUENCY INCREMENT (wavenumber)                 | 5 (=0.01 MICRON)                                  |                  |                |
| NUMBER ON PLOTS                                  | 1   |                  |                |
| HARD COPY OPTION                                 | 1-generate print / printer output                 |                  |                |
| INTERACTIVE GRAPHICS MODE                        | 6- 640x350 dot Mode                               |                  |                |
| PLOT TYPE  | 2-Plot Transmittance data vs Wavelength (Microns) |                  |                |
| LENGTH OF X AXIS (in inches)                     | 7 in  |                  |                |
| BEGINNING WAVENUMBER/wavelength( $\mu\text{m}$ ) | 665/1.00  |                  |                |
| ENDING WAVENUMBER/wavelength ( $\mu\text{m}$ )   | 10000/15.00                                       |                  |                |
| X-Axis Annotation Interval                       | 1   |                  |                |
| LENGTH OF Y AXIS (in inches)                     | 6 in  |                  |                |
| MINIMUM TRANSMITTANCE                            | 0   |                  |                |
| MAXIMUM TRANSMITTANCE                            | 1   |                  |                |
| Y-Axis Annotation Interval                       | 0.1   |                  |                |
| PLOT GRIDS                                       | 3-Course & Fine Grid                              |                  |                |
| PLOT TITLE                                       | GOOD  | TYPICAL-I        | BAD            |
| LINE TYPE  | 1 (normal line)                                   |                  |                |

### 6.5.2 Transmittance to Atmospheric Attenuation Coefficient Conversion

The transmittance values calculated from LOWTRAN were for a 1 km path length. Whereas, for missile target engagement simulation the transmittance values at different ranges are required. To calculate the transmittance for each target separately, the spectral transmittance data is converted to atmospheric attenuation coefficient ( $\sigma$ ). This is done using Equation 6-13:

$$\sigma = -\frac{\ln(\tau_a)}{R_{TMD}} \quad (6-13)$$

Where,

$\sigma$  is the atmospheric attenuation coefficient,

$\tau_a$  is the atmospheric transmittance, and

$R_{TMD}$  is the distance between the target and the missile seeker.

If at any wavelength, the value of transmittance ( $\tau_a$ ) is zero, then due to the logarithm the  $\sigma$  will go undefined (infinity). Therefore, before putting transmittance values in Equation 6-13, any zero transmittance value needs to be clipped to some very small value (e.g. MATLAB function “*eps*” which is  $2.22 \times 10^{-16}$  [MAT07]) so that the atmospheric attenuation coefficient at all wavelengths comes out to be a definite number.

### 6.5.3 Wave-numbers to Micrometers Conversion

LOWTRAN uses the wave-number for waveband measurements. The waveband selected is from 665 to 10000  $\text{cm}^{-1}$  which corresponds to approximately 15 to 1 micron respectively. The wave-number is converted to micrometers using Equation 6-14.

$$\lambda(\mu m) = \frac{10^4}{\text{Wavenumber}(\text{cm}^{-1})} \quad (6-14)$$

In LOWTRAN, the minimum wave-number increment is  $5 \text{cm}^{-1}$ . As the conversion is a reciprocal, the transmittance data corresponding to the wave-number is not at fixed intervals in microns. That means the  $5 \text{cm}^{-1}$  step near  $10000 \text{cm}^{-1}$  corresponds to about a 0.0005 micron interval. Whereas,  $5 \text{cm}^{-1}$  at  $665 \text{cm}^{-1}$  is a 0.112 micron increment. To achieve a fixed wavelength interval in microns, data interpolation techniques are used. To minimize the effects of the data interpolation error, the interval or the step size is kept as  $0.01 \mu\text{m}$  and the interpolation is done after the conversion of transmittance to attenuation coefficient, so that the interpolation error is not carried forward. Figure 6-12 shows the actual and interpolated transmittance data generated using MATLAB function “*interp1*” [MAT07]. The RMS error between the actual LOWTRAN data and the interpolated data is about 0.003 which is considered acceptable for IR signature modelling purpose.

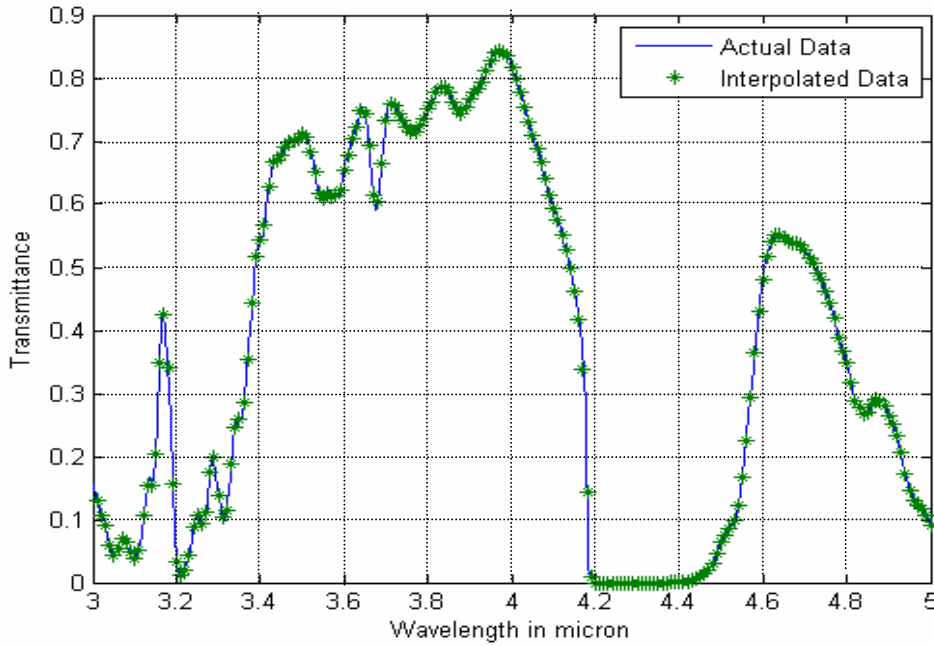


**Figure 6-12 : LOWTRAN actual data vs. interpolated data**

#### **6.5.4 Calculating Atmospheric Transmittance for each Target**

During the missile-target engagement simulation, the distance between the sensor and the target will continually change. Therefore, for each frame or time interval the atmospheric transmittance values are calculated as per the changing range by using Equation 6-15. Also, for more than one target, the transmittance values for each target are calculated as per their range.

$$\tau_a(\lambda) = e^{(-\sigma(\lambda)R_{TMD})} \quad (6-15)$$

#### **6.5.5 Scattering Effects of the Atmosphere**

Ideally, the atmospheric effects that need to be modelled are the absorption, scattering and turbulence. When the IR radiation passes through the atmosphere, a part of it is absorbed and a part is scattered. The total atmospheric attenuation coefficient  $\sigma(\lambda)$  has two components one  $\alpha(\lambda)$  the attenuation due to absorption and the other  $\gamma(\lambda)$  is due to atmospheric scattering. Equation 6-16 shows the components of the atmospheric attenuation coefficient.

$$\sigma(\lambda) = \alpha(\lambda) + \gamma(\lambda) \quad (6-16)$$

Initially, only the absorption properties of the atmosphere were considered. However, the scattering effects may be catered for by calculating atmospheric transmittance using LOWTRAN with multiple scattering.

Turbulence in the atmosphere is due to the time-varying temperature inhomogeneities which may result in blurring and distortion of the images. The affect of turbulence on electro-optical system is most pronounced for coherent systems (lasers). Turbulence affects imaging not only by visible sensors but also by the IR sensors. It is especially noticeable when viewing small objects at long distances [DRI99].

### 6.5.6 Modelling Atmospheric Path-radiance

The total spectral radiance calculated for targets, exhaust gas plume, flare and background after atmospheric attenuation may be generalized as shown in Equation 6-17.

$$N_{total}(\lambda) = N_{source}(\lambda) \cdot \tau_{path}(\lambda) \quad (6-17)$$

Where,  $N_{total}(\lambda)$  is the radiance after atmospheric attenuation,

$N_{source}(\lambda)$  is the radiance of the object,

$\tau_{path}(\lambda)$  is the atmospheric transmittance of the path length in between.

As the atmosphere comprises of particles, they thermally emit radiation along the path in the LOS from the source to the detector. Hence for higher order modelling, the path-radiance component  $N_{path}(\lambda)$  may be added to the above Equation 6-17. Therefore, the total spectral radiance received at the detector is shown as Equation 6-18.

$$N_{total}(\lambda) = N_{source}(\lambda) \cdot \tau_{path}(\lambda) + N_{path}(\lambda) \quad (6-18)$$

There are two ways for calculating the path-radiance of the atmosphere. The first method is by considering the atmospheric particles as blackbodies at a particular temperature [DRI99]. Equation 6-19 shows the path-radiance of the atmosphere.

$$N_{path}(\lambda) = (1 - \tau_{path}(\lambda)) \cdot N_{BB}(T_a) \quad (6-19)$$

Where,  $N_{BB}(T_a)$  is the radiance of the atmosphere as a blackbody at a particular atmospheric temperature ( $T_a$ ). The atmospheric transmittance of the path ( $\tau_{path}$ ) for the required spectral band and range can be calculated by using LOWTRAN. The path-



radiance in Equation 6-19 becomes less dominant as the path transmittance gets higher (closer to 1). Therefore, for the case of the cold clear sky, the path-radiance may contribute less towards the total radiance. However, at high atmospheric temperatures or low atmospheric transmittance values, the path-radiance may contribute significantly towards the total radiance. Similarly, the path-radiance can be less significant for shorter path lengths as compared to longer paths.

Another possible approach for considering the path-radiance ( $N_{path}$ ) effects may be to calculate the path-radiance using LOWTRAN as mentioned in paragraph 6-2-2, but to cater for the changing distance between the target and the sensor during simulation, the path radiance needs to be calculated for changing path length at every time interval or frame. This could possibly be done by running the LOWTRAN code several times for different path lengths and storing the data sets into lookup tables. While running the simulation, the desired path-radiance data can then be extracted from the lookup tables. Presently, the effects of path-radiance are not considered; however, this approach may be tried in future work.

## **6.6 Modelling Missile IR Detector and Optics**

The generic seeker types are from non-imaging to full imaging. In my initial work, the seeker was modelled as non-imaging with targets represented as point source at some location within the missiles FOV. Subsequently, the imaging type IR seeker was modelled which could represent the entire scene within its field-of-view as a matrix of pixels. The detector spectral coverage could be any waveband between 1 to 15 micron. Initially, the imaging seeker is modelled as a 512x512 pixel detector. However, the resolution of detector can be reduced to 256x256 or 128x128 or may be increased to 1024x1024. The seeker optics characteristics such as FOV, solid angle and transmission and detector noise-equivalent power ( $NEP$ ) and signal-to-noise ratio ( $SNR$ ) are considered for calculating power received at the detector and to estimate the lock-on range. However, the spectral response of the seeker detector and the optics is not modelled. This could be done in future work.

### **6.6.1 Missile Input Parameters**

The missile parameters can input in two ways. Either by selecting input parameters from the pre-stored data sets or entering values manually. The following missile parameters are required for modelling the missile seeker.

- (a) Noise Equivalent Power ( $NEP$ ) of detector in  $W/Hz^{1/2}$ ,
- (b) Signal-to-noise ratio ( $SNR$ ) of the detector,
- (c) Diameter of seeker optics ( $D_o$ ) in millimetres,
- (d) Focal length ( $f$ ) of seeker optics in millimetres,
- (e) Transmission of seeker optics ( $t_{opt}$ ),
- (f) Detector size ( $d$ ) in millimetres,
- (h) Detector waveband limits ( $\lambda_{start}$  and  $\lambda_{stop}$ ) in micro-metres.

Table 6-6 shows four sets of missile input data stored in an Excel spreadsheet. These values do not correspond to any specific missile system. However, the input data of several missiles may be stored in the same spreadsheet.

**Table 6-6 : Missile input parameters**

|             | NEP<br>( $W/Hz^{1/2}$ ) | SNR | Do<br>(mm) | f<br>(mm) | $t_{opt}$ | d<br>(mm) | $\lambda_{start}$<br>( $\mu m$ ) | $\lambda_{stop}$<br>( $\mu m$ ) |
|-------------|-------------------------|-----|------------|-----------|-----------|-----------|----------------------------------|---------------------------------|
| Missile I   | 1.00E-10                | 3   | 60         | 1         | 0.7       | 0.1       | 8                                | 12                              |
| Missile II  | 1.50E-10                | 5   | 70         | 10        | 0.8       | 0.3       | 3                                | 5                               |
| Missile III | 2.00E-10                | 7   | 50         | 15        | 0.9       | 0.5       | 3                                | 5                               |
| Missile IV  | 2.50E-10                | 10  | 80         | 20        | 0.75      | 0.6       | 8                                | 12                              |

## 6.7 Calculating Power Received at the Detector

For the 3D virtual reality missile-target engagement simulation, the total radiance received at the detector from the target, background and flare in the IR scene is calculated after atmospheric attenuation. This total radiance is normalized and used to represent the appearance of the IR scene objects in the 3D virtual world. However, for the static 2D IR signature analysis, the power received at the detector is calculated which is used for estimating the lock-on range of the missile. Figure 6-13 shows an example of a scenario in which three targets are presented as point sources. All three targets are at different distances from the detector. The following paragraph explains the procedure for calculating the total power received at the detector using the example shown in Figure 6-13.

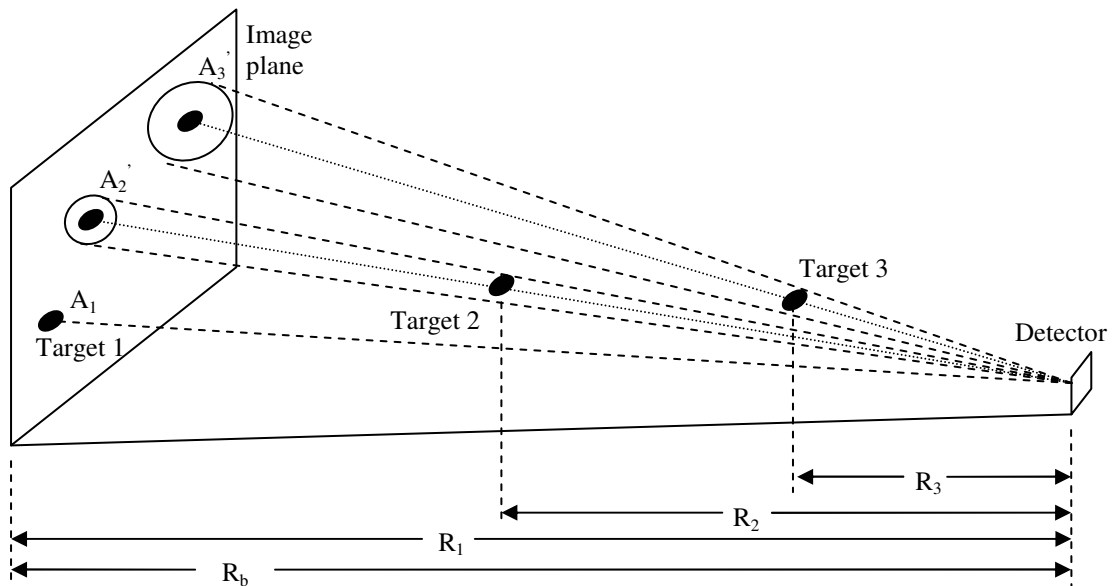


Figure 6-13 : Scenario with three targets at different ranges from seeker.

### 6.7.1 Calculating Projected Area of the Detector

The projected area ( $A_p$ ) of the detector is the area of the IR scene as viewed (or captured) by the detector optics. The projected area depends upon the detector size ( $d$ ), focal length ( $f$ ) and the slant range between the detector and the background ( $R_b$ ). Equation 2-13 of Chapter-2 is used to find the projected area of a square shape detector as given in Equation 6-20.

$$A_p = \left( \frac{d \cdot R_b \cdot 1000}{f} \right)^2 \quad (6-20)$$

Where,  $A_p$  is the projected area in meters square,

$d$  is the detector size in millimetres of a square detector,

$R_b$  is the distance from background to the detector in kilometres,

$f$  is the focal length in millimetres.

### 6.7.2 Calculating Solid-angle of Seeker Optics

The solid-angle ( $\Omega_{o,T}$ ) of the optics as seen from the target or the background can be calculated using Equation 2-11. To calculate the solid-angle the diameter of the optics and range of the target is required. The solid-angle for each target and background is calculated separately using Equation 6-21.

$$\Omega_{o,b} = \frac{\pi}{4} \left( \frac{D_o}{R_b} \right)^2 \quad (6-21)$$

Where,  $\Omega_{o,b}$  is the solid-angle of the optics as seen from the background, or in the case of the target, this is the solid-angle of the optics as seen from the target

$R_b$  is the range of the background, or in case of targets it is  $R_1$ ,  $R_2$  and  $R_3$

$D_o$  is the diameter of the optics.

### 6.7.3 Exposed Area of Targets as Projected on Background

To calculate the background area ( $A_b$ ), the exposed area of all the targets is to be subtracted from the projected area. In Figure 6-13, the area of the target No.1 ( $A_1$ ), (which is at the same distance as the background) will remain unchanged. However, target No.2 and target No.3 are in front of the background, therefore, the area of target No.2 and No.3 exposed on the background is more than their actual area. In Figure 6-13, the exposed area of target No. 2 and 3 ( $A_2'$  and  $A_3'$  respectively) are shown as circles around the actual area. To calculate the exposed area, the target No 2 and 3 are projected on to the background. The Equation 6-22 is derived by solving the similar triangles as shown in Figure 6-14(a) for the two sides of the area. Figure 6-14(b) shows the actual area ( $A_T$ ) and the exposed area ( $A_T'$ ).

$$A_T' = A_T \cdot \left( \frac{R_b}{R_T} \right)^2 \quad (6-22)$$

Where,  $A_T$  is the actual area of the target,

$A_T'$  is the exposed area of the target,

$R_b$  is the distance between detector and background,

$R_T$  is the distance between the target range and the detector.

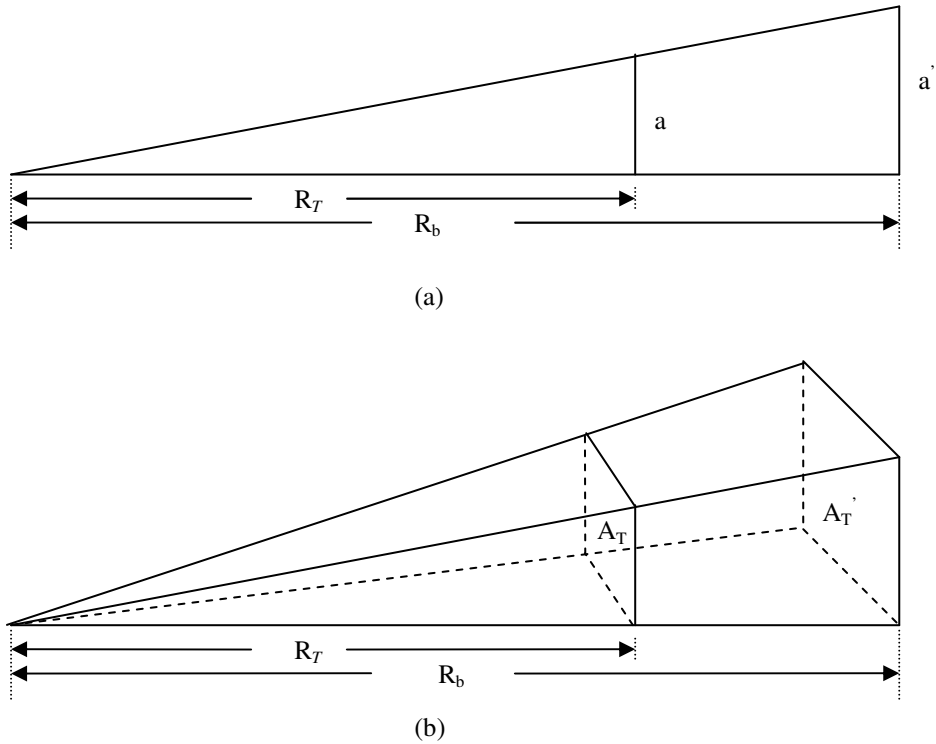


**Figure 6-14 : Target exposed area on the background**

#### 6.7.4 Point Source or Extended Source Target

For calculation of the lock-on range, it is important to decide whether the target is a point source or an extended source. This could be done by comparing the exposed area of the target and the projected area. If the exposed area of the target is less than the projected area of the seeker optics ( $A_T' < A_p$ ), the target is a point source, otherwise, it is an extended source target. In other words, any target which fills the entire FOV of the seeker is considered as an extended source target. The  $A_p$  and  $A_T'$  are calculated using Equation 6-20 and 6-22 respectively.

#### 6.7.5 Background Area

The power received at the seeker from the background is from the area which is not hidden behind the shadows of all the targets. The background area ( $A_B$ ) depends upon the projected area ( $A_p$ ) and the sum of the target areas as exposed on the background  $A_T'$ . In Figure 6-15 the three areas are shown with different texture. Equation 6-23 calculates the background area in presence of “ $n$ ” number of targets.

$$A_B = A_p - \sum_{i=1}^n A_{Ti}' \quad (6-23)$$

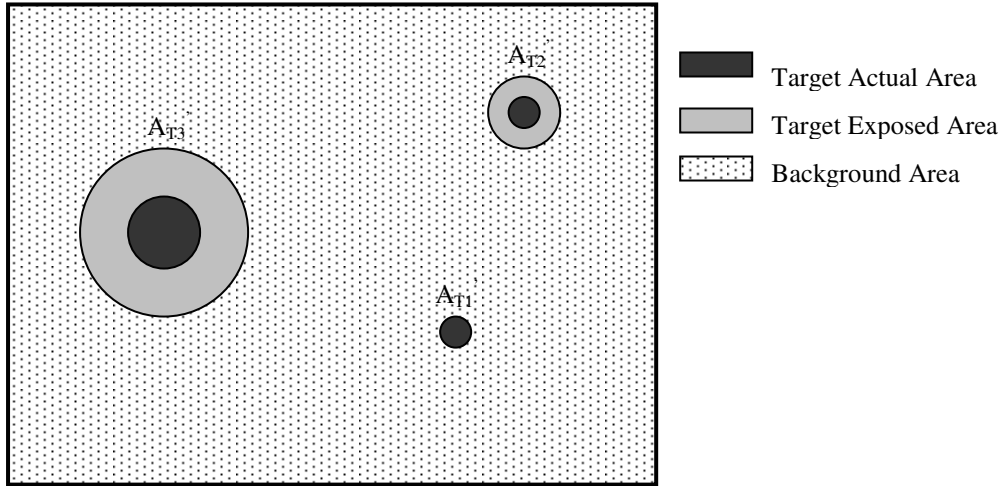


Figure 6-15 : Explaining background area

### 6.7.6 Power received at the Detector Due to Target and Background

The total power received at the detector once the targets are present is the sum of the power due to all the targets and the background which is not hidden behind the targets. To calculate the total power, first the power due to the targets and backgrounds is calculated separately. The total radiance of the targets after atmospheric attenuation was calculated at every 0.01 micron interval in Equation 6-3. The power per unit area received at the detector from each target is calculated using Equation 2-24. Similarly, the power per unit area for the background is calculated by Equation 6-25.

$$P_{tgt} / \text{unitarea} = \Omega_{O,T} \cdot t_{opt} \cdot \sum_{i=1}^n (N_{tgt_i} \cdot \tau_{a_i}) \quad (6-24)$$

$$P_b / \text{unitarea} = \Omega_{O,b} \cdot t_{opt} \cdot \sum_{i=1}^n (N_{b_i} \cdot \tau_{a_i}) \quad (6-25)$$

Where,

- $P_{tgt}$  is the power received at the detector due to the target,
- $P_b$  is the power received at the detector due to the background,
- $N_{tgt_i}$  is the radiance of the target at every 0.01 micron interval,
- $N_{b_i}$  is the radiance of the background at every 0.01 micron interval,
- $i$  denotes each 0.01 micron interval,
- $\tau_a$  is the atmospheric transmittance,
- $\Omega_{O,T}$  is the solid angle of the optics as seen by the target,

- $\Omega_{O,b}$  is the solid angle of the optics as seen by the background
- $t_{opt}$  is the transmittance of the seeker optics
- $n$  is the number of 0.01 micron intervals in the detector waveband

However, for further calculations, such as the lock-on range, the power per unit area is multiplied by the respective target area ( $A_T$ ) to get the total power due to each target [RIC02b] as shown in Equation 6-26.

$$P_{tgt} = \Omega_{O,T} \cdot t_{opt} \cdot A_T \cdot \sum_{i=1}^n (N_{tgt_i} \cdot \tau_{a_i}) \quad (6-26)$$

To calculate the total power due to the background, the background area  $A_B$  calculated in Equation 6-23 is multiplied with the power per unit area calculated in Equation 6-25.

$$P_b = \Omega_{O,b} \cdot t_{opt} \cdot A_B \cdot \sum_{i=1}^n (N_{B_i} \cdot \tau_{a_i}) \quad (6-27)$$

The total power  $P_T$  reached at the detector, once the targets are present, is the sum of the power due to all targets  $P_{tgt}$  as calculated in Equation 6-26 and the power due to the left over background  $P_b$  as calculated in Equation 6-27. The total power once the targets are present is given by Equation 6-28.

$$P_T = P_b + \sum_{i=1}^m P_{tgt_i} \quad (6-28)$$

Where, “ $m$ ” is the number of targets in the FOV.

Similarly, the background power ( $P_B$ ) received at the detector once there is no target present, is calculated by using the projected area as calculated in Equation 6-20 and the background radiance  $N_B$  is calculated in Equation 6-1.

$$P_B = \Omega_{O,b} \cdot t_{opt} \cdot A_P \cdot \sum_{i=1}^n (N_{B_i} \cdot \tau_{a_i}) \quad (6-29)$$

### 6.7.7 Lock-on Range or Maximum Range Prediction

For any target to be detected, the difference of powers received at the seeker once the target is present and that of background alone must be more than the minimum detectable power of the detector which is the product of Noise Equivalent Power (*NEP*) and the signal-to-noise ratio (*SNR*).

$$P_T - P_B \geq NEP \cdot SNR \quad (6-30)$$

Putting the values of target power  $P_T$  and the background power  $P_B$  from Equation 6-28 and Equation 6-29 respectively, in Equation 6-30, an expression for the lock-on range of the missile seeker is derived [RIC02b].

$$R_{Lock-on} = \sqrt{\frac{\pi(N_{tgt} - N_B) \cdot A_T \cdot D_o^2 \cdot \tau_a \cdot t_{opt}}{4 \cdot SNR \cdot NEP}} \quad (6-31)$$

$$\tau_a = e^{-\sigma(\lambda) \cdot R} \quad (6-32)$$

However, from Equation 6-32, the atmospheric transmittance  $\tau_a$  is also a function of the range. This would make it impossible to write an equation for lock-on range in a closed-form. Therefore, the lock-on range can be calculated using any numerical method for solving non-linear equations. The Equation 6-31 and 6-32 are solved by using the Newton Raphson numerical method for solving non-linear equations [KRE75].

### 6.7.8 Fidelity of the Model

In this work, the word fidelity was used in twofold meanings: “accuracy” and “realism”. The accuracy relates to the mathematical modelling that means how close or accurate the results are to the actual measured readings. Whereas, the realism is in terms of the image quality, that means how close to reality or how realistic the scene looks, if compared with the actual scene. The fidelity of the model depends upon the intended use. For the visual observations by the human eye, the low-fidelity may be



considered sufficient. For missile seeker detection, the medium or high-fidelity may be required. To keep the model simple, at some times even the low-fidelity and low-accuracy may be adequate for a specific purpose so to increase the fidelity becomes unnecessary [KIS99].

One of the objectives of my thesis is to develop a high fidelity model. I started with the first order low-fidelity model and the fidelity was stepwise improved to achieve as accurate and as close to reality as possible. Initially, only one target with uniform temperature and emissivity was considered. The target was represented by the radiance as seen or observed at the target. Then the number of targets or sub-targets was increased and now any number of sub-targets can be modelled. Initially, only the emissive properties of the target were modelled. Then reflection and transmission are also considered. The exhaust gas plume, leading edge reflection and cold sky reflections from the glass canopy are modelled. Initially, no countermeasures were modelled and now multiple flare dispensation with spectral and temporal responses is modelled. Initially, the background was modelled as one uniform temperature and emissivity object. Now, multiple backgrounds as sky and ground are modelled. The atmospheric effects were not considered initially, and then the atmospheric transmittance was modelled as a simple exponential decay as a function of the distance between the target and the seeker. The atmospheric attenuation coefficient was modelled by giving any number from 0 to 1 to represent the good or bad weather conditions. Finally, the LOWTRAN atmospheric transmission code was used to model the atmospheric transmittance. For 3D virtual reality missile target engagement simulations, the targets and the background are represented by the radiance after atmospheric attenuation. Whereas, for 2D static analysis the power received at the seeker detector is calculated to estimate the lock-on range.

## **6.8 Data Stored in Excel Spreadsheets**

Ideally, for keeping the simulation planning and input process simple, a Graphical User Interface (GUI) may be developed. However, the Microsoft Excel spreadsheet is used for storing all the inputs and LOWTRAN transmittance and sky radiance data outside the main programme. The required data may be called in the main programme using MATLAB “*xlsread*” function [MAT07]. For IR signature modelling and simulation the following data sets are stored in Microsoft Excel spreadsheets:

- (a) Target or sub-targets input parameters,
- (b) Flare input parameters,
- (c) Missile input parameters,
- (d) Background input parameters,
- (e) Atmospheric transmittance data,
- (f) Sky radiance data.

Presently, the input parameters for a few targets, flares, backgrounds and missiles are stored in the Excel spread sheet. However, more data sets could easily be stored in the same spreadsheets. The atmospheric transmittance and sky radiance data for three weather conditions and different altitudes are stored in spreadsheets. The data for several more weather conditions and altitudes may be calculated using LOWTRAN code and stored in the same spreadsheets.

## **6.9 Source Code of the Main Algorithm**

The MATLAB is used for the IR signature mathematical modelling and simulation. The complete source code of the main programme, sub-programmes for extraction of LOWTRAN data and the other are copied on a CD provided with the thesis report.

## **6.10 Conclusion**

The IR signature model includes realistic radiometric targets, background, atmospheric effects and countermeasures. An effort is made to develop high-fidelity, first-principle models using MATLAB computational software and LOWTRAN atmospheric transmission code. As an initial effort, to implement the theoretical concepts into a model, a very simple and low Fidelity IR signature model was developed. Subsequently, the fidelity is step-by-step increased by adding various features. The military targets are modelled as sub-targets on the basis of their thermal and radiometric properties. The exhaust gas plume inviscid core is modelled as two co-centric cones with different temperatures. The IR countermeasures flare spectral and temporal responses are modelled. The background is modelled as sky or ground or both with different layers. The sky radiance and atmospheric transmittance data are calculated for different weather conditions and altitudes using LOWTRAN code. The spectral band of 1 to 15  $\mu\text{m}$  is modelled with step size of 0.01  $\mu\text{m}$ . For the IR

signature of a 3D virtual reality animation, the total radiance of sub-target, exhaust gas plume, glass canopy, flares and the background after atmospheric attenuation is represented by different false colours and shininess and transparency. For the 2D static analysis the power received at the detector is calculated for estimating the lock-on range.

